columns, while in β-$\mathrm{V_3S}$ they form nets. This is apparent from Fig. 6 and one can easily see how the metal atoms in the β-W structure must be moved to give the atomic arrangement in β-$\mathrm{V_3S}$ (the V–B columns have been omitted for the sake of clarity). It seems reasonable to suppose that this rearrangement causes little change in bond distance between the metal atoms in the V–V column. It is between these metal atoms that the short bond distance is observed in the β-W structure, and it is also between these atoms that the short V–V distance, 2·44 Å, is found in β-$\mathrm{V_3S}$.

The structures of α-$\mathrm{V_3S}$ and $\mathrm{Ni_3P}$ are closely related, but α-$\mathrm{V_3S}$ has higher symmetry than $\mathrm{Ni_3P}$. It might therefore seem natural to describe the structure of $\mathrm{Ni_3P}$ as a somewhat deformed α-$\mathrm{V_3S}$ structure. The $\mathrm{Ni_3P}$ structure is related to the β-W structure via the structures of α-$\mathrm{V_3S}$ and β-$\mathrm{V_3S}$. That such a relationship might be expected is indicated by the remarks of Schønberg (Aronsson, 1955) that $\mathrm{V_3P}$ is isotypic with $\mathrm{Ni_3P}$, and by Mathias *et al.* (1957) that $\mathrm{V_3P}$ has a slightly distorted β-W structure.

The authors wish to thank Prof. Haakon Haraldsen for his interest in this study and for placing laboratory facilities at their disposal.

References

Aronsson, B. (1955). *Acta Chem. Scand.* **9**, 137.
Biltz, W. & Köcher, A. (1939). *Z. anorg. Chem.* **242**, 275.
Cruickshank, D. W. J. (1949). *Acta Cryst.* **2**, 65.
Geller, S. (1956). *Acta Cryst.* **9**, 885.
Internationale Tabellen zur Bestimmung von Kristallstrukturen (1935). Berlin: Borntraeger.
International Tables for X-ray Crystallography (1952). Birmingham: Kynoch Press.
Mathias, B. T., Wood, E. A., Corenzwit, E. & Bala, V. B. (1957). *J. Phys. Chem. Solids*, **1**, 188.
Pauling, L. (1957). *Acta Cryst.* **10**, 374.
Pauling, L. (1947). *J. Amer. Chem. Soc.* **69**, 542.
Pedersen, B. (1958). Thesis. University of Oslo.
Seybolt, A. U. & Sumsion, H. T. (1953). *J. Metals*, **5**, 292.
Vogel, R. & Wüstefeld, A. (1938). *Archiv Eisenhüttenw.* **12**, 261.

Acta Cryst. (1959). **12**, 1027

X-ray Studies on the Metal Complexes with the Glyoximes. II.
Structure of the Pt-Dimethyl-Glyoxime

By Edoardo Frasson, Carlo Panattoni and Roberto Zannetti

Centro di Strutturistica Chimica del C. N. R. and Istituto di Chimica Organica, Universita' di Padova, Italia

(*Received* 1 *April* 1959 *and in revised form* 7 *May* 1959)

During a systematic investigation of the metal complexes of the glyoximes, the structure of Pt-dimethyl-glyoxime has been examined. It has the same space group *Ibam* as Ni-dimethyl-glyoxime. The lattice constants are $a = 16{\cdot}73$, $b = 10{\cdot}59$, $c = 6{\cdot}47$ Å; $Z = 4$. Such values are similar to those found in Ni-dimethyl-glyoxime.

The molecule is planar and the Pt–Pt distances between metallic atoms of overlying molecules are 3·23 Å. The intramolecular distance of 3·03 Å between the oxygen atoms bound by a hydrogen bond, is significantly longer than the one in Ni-dimethyl-glyoxime (2·44 Å) and in Cu-dimethyl-glyoxime (2·57–2·70 Å).

Introduction

In this Centro di Strutturistica Chimica we have examined a series of compounds having the following general formula:

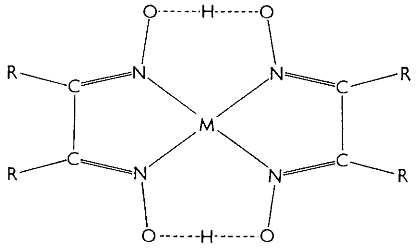

This work has shown a variety of possibilities of packing as well as of molecular structure due to the differences of coordination of the metals as well as to the substituent group R present in the molecule.

Frasson, Bardi & Bezzi (1959) have recently described the structure of Cu-dimethyl-glyoxime showing the differences between it and the Ni-dimethyl-glyoxime studied by Godycki & Rundle (1953). The two structures are mainly differentiated by the pyramidal five-fold coordination of the copper, the lack of planarity of the molecule, the formation of a dimer through Cu–O bonds between atoms of different molecules on the one hand and the regular octahedral coordination of the Ni, the planarity of the molecule and the formation of molecular chains through Ni–Ni bonds on the other.

During our preliminary examination of the structures of methyl–ethyl–glyoximes of Cu and Ni (1959), two new structural types were detected for the compounds with octahedral coordination distorted for the Cu and regular for the Ni respectively, and with formation of molecular chains through M–O bonds between atoms of different molecules.

The structure of Pt–dimethyl–glyoxime, described in the present paper, is seen to belong to the same structural type as Ni–dimethyl–glyoxime.

Experimental and crystal data

Pt–dimethyl–glyoxime crystals were prepared from chloro–platinic acid reduced with SO_2 and dimethyl–glyoxime in alcoholic solution. The dark-grey compound was purified through several crystallizations from nitrobenzene. The brown crystals were examined with Cu $K\alpha$ radiation in the precession camera for space-group determination. The crystals proved to belong to the space-group *Ibam*. The lattice constants were:

$$a = 16{\cdot}73 \pm 0{\cdot}06, \quad b = 10{\cdot}59 \pm 0{\cdot}05, \quad c = 6{\cdot}47 \pm 0{\cdot}02 \text{ Å};$$

the pycnometric density is 2·40 g.cm.$^{-3}$; the calculated density for $Z = 4$ is 2·40 g.cm.$^{-3}$.

The intensities were measured by the multiple-film technique in a Weissenberg camera having an attachment for linear integration. Intensities were evaluated by means of photometric integration.

Notwithstanding the appreciable value of the mass absorption coefficient, the absorbing power of our crystals appeared to be very low owing to their small size. The values of the absorption coefficient in the direction of the two diagonals of the section were $\mu l = 1{\cdot}47$ and $\mu l = 1{\cdot}07$ and in the third direction $\mu l = 1{\cdot}32$. The intensities were corrected with the usual Lorentz and polarization factors.

Electron-density maps

Owing to the presence of only four molecules in the unit cell, the Pt atom is to be located at the symmetry centres. Projections of electron density were therefore directly calculated on (001) and (010). The structure factors were given the positive sign owing to the presence of the heavy atom at the cell origin.

From the electron-density projections it is seen that the molecules are parallel to the (001) plane with coordinates 0 and ½ along the z direction. The projection shows the characteristic diffraction ripples due to the heavy atom. In order to measure the probable displacement caused by the diffraction ripples on the localisation of the light atoms, we examined the cross-section of the electron density in a radial direction with respect to the heavy atom centre in a zone with no maxima due to light atoms. The first order ring has the value 8 e.Å^{-2}. This diffraction effect being far from all maxima due to light atoms, no disturbance is possible. The second-order ring, having the value 1·8 e.Å^{-2}, slightly disturbes the position of the two nitrogen atoms, the maximum height of which reaches 16 e.Å^{-2}. The third-order ring has the value of 1·2 e.Å^{-2} in a zone where the maxima due to the oxygen atoms and to the carbon atoms of the chelate ring are 16 e.Å^{-2}. In both cases the small contribution due to these spurious maxima were subtracted from the electron density in order to localize the light atoms.

The structure factors were calculated with the atomic coordinates determined from the electron-density map. For the overlapping maxima the knowledge of the bonds lengths and angles of similar compounds were used in a first approximation. The atomic factors of Berghuis *et al.* (1955) and the mean temperature factor derived from a plot of the log F_o/F_c against $\sin^2\theta/\lambda^2$ were used to calculate the contribution of the light atoms.

For the calculation of the atomic factor of the heavy atom, the calculated contribution of the light atoms was subtracted from the experimental structure factors and a plot was drawn with the values $F_o - F_{\text{C, N, O}}$ against $\sin^2\theta/\lambda^2$. The curve obtained is shown in Fig. 1. At this stage the reliability factor was $R = 0{\cdot}14$.

Examination of the profile of the electron-density maxima revealed the existence of a thermal factor for the light atoms quite different from the mean thermal factor. By introducing this new thermal factor for the light atoms the reliability factor fell to $R = 0{\cdot}11$.

The calculation of some $F_o - F_c$ maps suggested some displacements of light atoms. For example, the O_1 atom that initially had been localised using an angle Pt–N_1–O_1 of 120° was displaced away from the O_2 atom so that the final value of the angle Pt–N_1–O_1 became 134°. This value is in agreement with the Pt–N_2–O_2 angle of 135° independently determined.

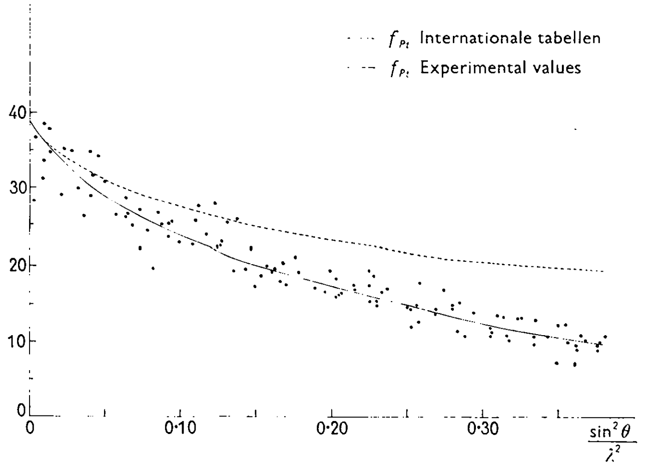

Fig. 1. Diffraction power of the Pt atom in Pt-dimethyl-glyoxime as a function of $\sin^2\theta/\lambda^2$. The atomic scattering factor given by *Internationale Tabellen* are also shown for comparison.

Table 1. *Observed and calculated structure factors for the hk*0 *and h*0*l reflections*

*hk*0	F_o	F_c
200	356·9	354·8
400	248·2	240·2
600	250·0	261·0
800	240·0	247·4
10,0,0	186·6	191·3
12,0,0	197·6	190·5
14,0,0	135·4	125·7
16,0,0	120·7	111·0
18,0,0	102·7	112·4
20,0,0	58·5	95·9
110	376·0	384·2
310	220·1	195·1
510	310·4	294·9
710	319·1	279·0
910	216·4	208·2
11,1,0	178·6	181·1
13,1,0	145·1	164·2
15,1,0	127·5	128·1
17,1,0	111·0	126·4
19,1,0	85·2	93·5
21,1,0	82·0	76·9
020	229·6	235·8
220	200·3	190·7
420	197·6	184·9
620	301·2	274·0
820	232·2	232·4
10,2,0	195·8	218·7
12,2,0	153·4	159·0
14,2,0	137·7	128·5
16,2,0	119·3	125·4
18,2,0	93·4	110·0
20,2,0	75·1	79·7
130	299·3	278·2
330	244·6	226·0
530	179·6	169·9
730	210·8	196·8
930	195·7	183·9
11,3,0	181·9	170·9
13,3,0	104·5	107·3
15,3,0	128·0	115·1
17,3,0	113·2	108·0
19,3,0	80·6	96·2
040	213·2	248·9
240	305·4	312·9
440	239·9	219·0
640	179·2	193·5
840	165·3	177·7
10,4,0	220·1	177·7
12,4,0	131·7	128·2
14,4,0	123·8	121·0
16,4,0	111·4	116·4
18,4,0	82·0	95·4
20,4,0	78·2	78·8
150	231·2	246·0
350	239·0	245·8
550	163·0	172·8
750	182·9	191·8
950	230·2	223·3
11,5,0	174·1	176·0
13,5,0	125·8	131·9
15,5,0	125·7	122·9
17,5,0	92·6	104·2
19,5,0	83·0	88·8
060	186·5	198·3
260	209·1	204·4
460	226·5	214·1
660	209·1	193·3
860	254·2	210·7
10,6,0	186·0	168·2
12,6,0	127·5	127·4
14,6,0	118·4	122·3
16,6,0	102·7	111·0
18,6,0	76·0	94·0
170	206·3	188·9
370	198·9	193·0
570	192·0	170·8
770	150·2	160·0
970	151·9	154·5
11,7,0	104·0	96·5
13,7,0	111·8	107·7
15,7,0	100·4	101·9
17,7,0	76·9	90·2
080	180·6	190·7
280	179·6	165·2
480	133·1	132·2
680	134·4	116·7
880	157·9	146·6
10,8,0	114·7	122·3
12,8,0	98·1	103·3
14,8,0	92·1	97·3
16,8,0	80·2	80·2
190	156·6	141·4
390	123·4	131·1
590	127·5	120·6
790	141·4	132·7
990	135·4	132·7
11,9,0	118·8	110·1
13,9,0	94·9	103·6
15,9,0	77·8	93·5
0,10,0	149·2	130·1
2,10,0	152·4	137·9
4,10,0	130·4	123·2
6,10,0	152·8	130·6
8,10,0	126·1	119·6
10,10,0	114·1	109·3
12,10,0	94·9	92·2
14,10,0	67·2	88·1
1,11,0	149·6	138·1
3,11,0	123·8	129·6
5,11,0	120·7	120·2
7,11,0	112·8	113·2
9,11,0	88·9	101·1
11,11,0	77·4	94·4
0,12,0	108·1	107·0
2,12,0	106·4	105·2
4,12,0	104·4	104·0
6,12,0	98·1	100·8
8,12,0	74·6	94·3
1,13,0	76·0	95·3
3,13,0	66·3	84·2
5,13,0	63·1	82·6

*h*0*l*	F_o	F_c
002	567·1	567·1
202	299·2	303·2
402	200·0	216·8
602	236·5	231·6
802	234·9	221·7
10,0,2	154·2	179·7
12,0,2	153·0	171·3
14,0,2	115·3	117·1
16,0,2	79·5	100·8
18,0,2	83·5	103·6
004	317·3	331·4
204	230·9	212·4
404	158·6	171·0
604	176·5	176·5
804	190·8	169·8
10,0,4	115·3	145·1
12,0,4	130·6	137·6
14,0,4	90·8	100·5
16,0,4	72·3	91·4
006	195·3	196·0
206	145·3	142·9
406	130·5	124·1
606	143·3	124·2
806	120·5	121·9
10,0,6	81·5	106·8
12,0,6	89·1	104·1
14,0,6	74·7	80·2
008	135·7	120·9
208	78·7	96·0
408	87·9	86·7
608	81·9	86·4
808	78·3	84·8
10,0,8	65·4	76·0

The comparison between F_o and the new F_c gave $R=0{\cdot}09$. A maximum close to the origin of the F_o-F_c maps was interpreted as due to thermal anisotropy of the heavy atom. An anisotropic thermal factor was introduced in the contribution of the Pt atom with the formula:

$$f_r=f_o.\exp\left[-(A+B\cos^2\varphi)\sin^2\theta/\lambda^2\right]$$

where the coefficient A is the thermal factor derived from the experimental data in the direction of minimum vibration and $A+B$ is the temperature factor derived from the experimental data in the direction of maximum vibration.

With this correction R was lowered to a final value of 0·07.

In the projection on (010) the comparison between F_o and F_c was calculated with the known coordinate x/a and with $z/c=0$ and with the introduction of the temperature factors derived from the other projection. The reliability factor was 0·07. Table 1 lists experimental and calculated structure factors for the *hk*0 and *h*0*l* zones.

Accuracy

Notwithstanding the high difference in the atomic number between the Pt and the other atoms in the structure the maxima due to oxygen and nitrogen atoms are sufficiently smooth and regular. On the contrary the maxima due to the methyl-group are spread and irregular. This may be seen in Fig. 2 in which the projection of electron density on (001) is drawn.

Unfortunately the nitrogen atoms of two overlying molecules give overlapping maxima in the projection.

Maxima of oxygen atoms also overlap those of the carbon atoms of the chelate ring. Therefore it was not possible to calculate the standard error of the coordinates using Cruickshank's method.

Determination of the mean error of coordinates by Luzzati's method obviously cannot be used owing to

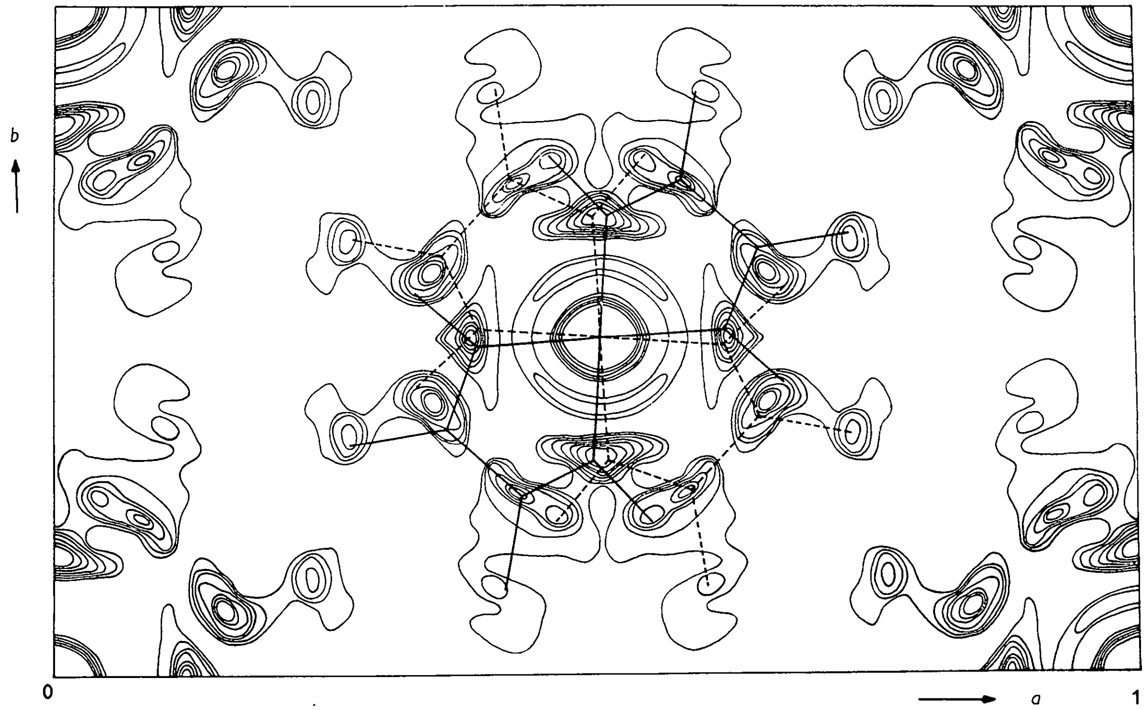

Fig. 2. Electron-density projection on (001) for Pt-dimethyl-glyoxime. Contours are at intervals of 2 e.Å^{-2} for the light atoms and of 4 e.Å^{-2} for the Pt atom starting from 4 e.Å^{-2}. Upper levels for the Pt-atom are omitted.

the presence of a very heavy atom at a centre of symmetry. Therefore we have calculated a probable error by merely geometrical considerations of the shape of the maxima in the electron-density projection. Table 2 lists atomic coordinates with the probable errors. In Table 3 the bonds lengths and angles are listed.

Table 2. *Atomic coordinates and probable errors*

	x/a	y/b	z/c
Pt	0·000	0·000	0·000
C_1	0·234 ± 0·003	0·144 ± 0·005	0·000
C_2	0·148 ± 0·003	0·120 ± 0·005	0·000
C_3	0·084 ± 0·003	0·224 ± 0·005	0·000
C_4	0·097 ± 0·003	0·361 ± 0·005	0·000
N_1	0·115 ± 0·002	0·012 ± 0·003	0·000
N_2	0·007 ± 0·002	0·184 ± 0·003	0·000
O_1	0·172 ± 0·002	−0·073 ± 0·003	0·000
O_2	−0·042 ± 0·002	0·268 ± 0·003	0·000

Table 3. *Bond lengths and angles*

Pt–Pt	3·23 ± 0·01 Å		
Pt–N_1	1·93 ± 0·04	Pt–N_2	1·95 ± 0·04 Å
N_1–O_1	1·31 ± 0·06	N_2–O_2	1·24 ± 0·06
N_1–C_2	1·27 ± 0·09	N_2–C_3	1·38 ± 0·09
C_2–C_3	1·57 ± 0·10		
C_1–C_2	1·46 ± 0·10	C_3–C_4	1·47 ± 0·10
O_1–O_2	3·03 ± 0·06		
N_1–Pt–N_2	83°		
Pt–N_1–O_1	134	Pt–N_2–O_2	135°
Pt–N_1–C_2	120	Pt–N_2–C_3	115
O_1–N_1–C_2	106	O_2–N_2–C_3	110
N_1–C_2–C_3	113	N_2–C_3–C_2	117
N_1–C_2–C_1	126	N_2–C_3–C_4	117
C_1–C_2–C_3	121	C_2–C_3–C_4	126

Description of the structure and discussion

Fig. 3 shows the Pt–dimethyl–glyoxime molecule with the bond lengths and angles calculated from the atomic coordinates. The structure is similar to the Ni–dimethyl-glyoxime structure with octahedral coordination around the Pt atom.

The length of the *M–M* bond normal to the plane of the molecule is 3·23 ± 0·01 Å. In Fig. 4 the molecular contacts caused by this intermolecular bond are shown.

The hydrogen bond in this structure is remarkably weaker than the O–H–O bond in the other structure of this type.

As is shown in Table 4, the lengths of the Pt–N bonds are not very different from the lengths of the

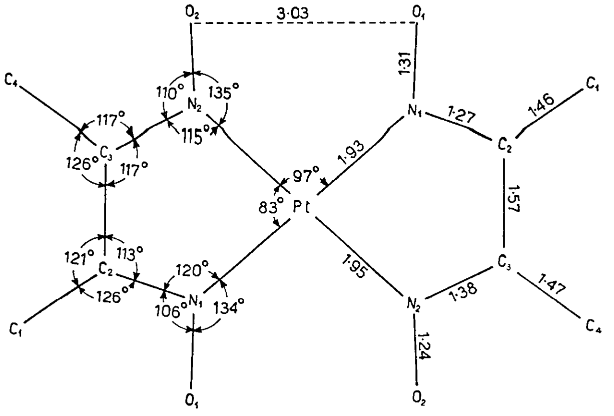

Fig. 3. Bond lengths and angles in Pt-dimethyl-glyoxime.

Table 4. *Variation of the M–*N *bonds and of hydrogen bonds in the glyoxime complexes*

Compound	*M*–N bond (Å)	O–H–O bond (Å)	*M*–N–O angle
Cu-dimethyl-glyoxime	1·91; 1·96	2·53; 2·70	121° 30′; 125°
Ni-dimethyl-glyoxime	1·87; 1·90	2·44	118°; 122°
Pt-dimethyl-glyoxime	1·93; 1·95	3·03	135°

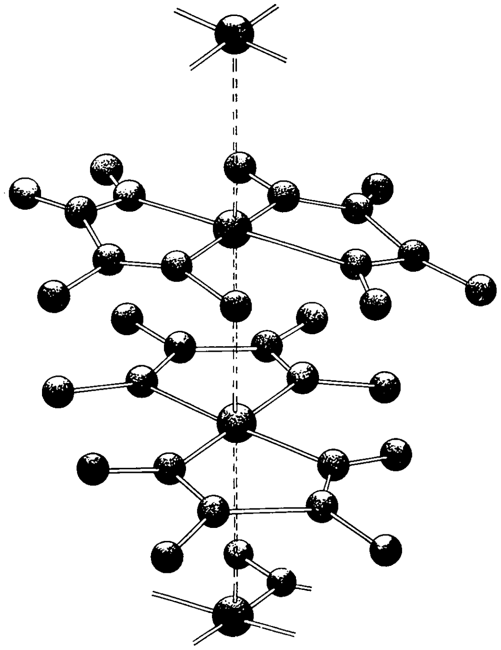

Fig. 4. Perspective view of the molecular contacts in Pt-dimethyl-glyoxime.

M–N bonds in Ni-dimethyl-glyoxime and in Cu-dimethyl-glyoxime. Therefore the exceptional length of the hydrogen bond in this structure is due to an increase of the Pt–N–O angles in respect to the *M*–N–O angles in the other complexes of this type.

From an infrared spectroscopic investigation of this compound in the solid state it was shown that the O–H stretching frequency for the hydrogen bond is about 3450 cm.$^{-1}$. According to the empirical correlation found by Nakamoto, Margoshes & Rundle (1955), this value corresponds to a hydrogen bond length of about 2·9 Å. The difference of 0·1 Å from the X-ray data is of the order of the uncertainty of the method of Nakamoto *et al.* (1955).

A discussion will be presented elsewhere on the spectroscopic data of this compound in relation to the other complexes of the series *M*–*R*–*R*′-glyoximes.

We are indebted to Dr Cesare Pecile and to Istituto di Chimica Fisica of the University of Padua for the spectroscopic data.

References

Berghuis, J., Haanappel, IJ. M., Potters, M., Loopstra, B. O., McGillavry, C. H. & Veenendaal, A.L. (1955). *Acta Cryst.* **8**, 478.

Frasson, E., Bardi, R. & Bezzi, S. (1959). *Acta Cryst.* **12**, 201.

Frasson, E., Panattoni, C. & Zannetti, R. (1959). *Ric. Sci.* **29**, 744.

Godycki, L. E. & Rundle, R. E. (1953). *Acta Cryst.* **6**, 487.

Nakamoto, K., Margoshes, M. & Rundle, R. E. (1955). *J. Amer. Chem. Soc.* **77**, 6480.